# FREE CONVECTIVE HEAT TRANSFER FROM AN OBJECT AT LOW RAYLEIGH NUMBER

**Md. Golam Kader** and **Khandkar Aftab Hossain***
Department of Mechanical Engineering,
Khulna University of Engineering & Technology, Khulna 9203, Bangladesh.
*Corresponding e-mail: aftab@me.kuet,ac.bd

***Abstract:*** *Free convective heat transfer from a heated object in very large enclosure is investigated in the present work. Numerical investigation is conducted to explore the fluid flow and heat transfer behavior in the very large enclosure with heated object at the bottom. Heat is released from the heated object by natural convection. Entrainment is coming from the surrounding. The two dimensional Continuity, Navier-Stokes equation and Energy equation have been solved by the finite difference method. Uniform grids are used in the axial direction and non-uniform grids are specified in the vertical direction. The differential equations are discretized using Central difference method and Forward difference method. The discritized equations with proper boundary conditions are sought by SUR method. It has been done on the basis of stream function and vorticity formulation. The flow field is investigated for fluid flowing with Rayleigh numbers in the range of* $1.0 \leq Ra \leq 1.0\times10^3$ *and Pr=0.71. It is observed that the distortion of flow started at Rayleigh number Ra=10. It is observed that the average heat transfer remains constant for higher values of Reyleigh number and heating efficiency varies with Ra upto the value of Ra=35 and beyond this value heating efficiency remains constant.*

***Keywords:*** *Free convection, enclosure, distortion, Rayliegh no., vorticity.*

## INTRODUCTION

Free convection heat transfer from a heated body draws additional attention to the researchers, because it does not require any external energy for transferring heat. Only the variation of density of fluid plays important role to transfer heat from the body. The present work deals with free convection heat transfer from a heated body in a very large enclosure in quiescent atmospheric condition. Buoyancy induced flow and heat transfer is an important phenomenon in engineering systems due to its wide applications in electronic cooling, heat exchangers, double pane windows, molding and casting, nuclear and chemical reactors, flooding protection for buried pipes, solidification processes, growing crystals and solar collectors etc [1].

Oh et al. [2], used a numerical simulation to study natural convection in a vertical square enclosure containing heat generating conducting body, when a temperature difference existed across the enclosure. The streamlines, isotherms and average Nusselt number at the hot and cold walls are presented and discussed. Roychowdhury et al. [3], analyzed the natural convective flow and heat transfer features for a heated cylinder kept in a square enclosure with different thermal boundary conditions. Arnab et al. [4], performed an extensive analysis of flow pattern and heat transfer from a heated rectangular cylinder enclosed inside an enclosure with three different aspect ratio. The effect of aspect ratio and two kinds of boundary conditions (i.e, constant wall heat flux and constant wall temperature) were studied. They concluded that the uniform wall temperature heating was greatly different from the uniform wall flux heating. Jami et al. [5], analyzed natural convection heat transfer in a differentially heated enclosure, within which a centered, circular, heat-conducting body generates heat. They concluded that for a constant Rayleigh number, the average Nusselt number at the hot and cold walls varied linearly with temperature-difference ratio.

Sidik et al. [6], studied numerically, the fluid flow behavior and heat transfer mechanism from a heated square cylinder located at various heights inside a square enclosure by the numerical method in the range of $103 \leq Ra \leq 106$. Their computational results proved that the flow pattern, number, size and formation of vorticies and also heat transfer mechanism were critically dependent on Rayleigh number and the position of heated square cylinder in enclosure. Hussain et al. [7], considered the problem of natural convection in a square enclosure which had an isothermal walls and was heated by a concentric internal circular isoflux boundary. They concluded that vorticies down the bottom and up the top of the inner cylinder can be noticed as the inner cylinder moved upward and downward. However, a very little literatures deal with natural convection problem when a conductive circular cylinder with heat generation embedded inside a square enclosure and moves at different locations along the enclosure diagonal. The objective of this study is to simulate two-dimensional free convection heat transfer in a cylinder within a square enclosure in order to investigate the effect of a hot conductive circular cylinder location and its heat generation on the heat transfer and fluid flow in an enclosure. R. T. Bailey et al. [8], investigated the force convective heat transfer relations for atmospheric flow over sparsely

vegetated areas and compared to existing relations for flow in rough ducts. Experimental convection coefficients obtained are compared to the analytical relations. Convection coefficient is directly calculated by measuring the power dissipation and surface temperatures. The experimental heat transfer results are correlated with micrometeorological models from which a soil roughness height is calculated. A simplified heat transfer correlation is presented for desert surfaces.

The Grashof no. is calculated from $Gr = g\beta\Delta\theta W^3/\nu^2$ and Prandtl no. is calculated from $\Pr = \nu/\alpha$. The Rayleigh no. *Ra* = GrPr $= g\beta\Delta\theta W^3/\nu\alpha$. The Nusselt number, Nu at the hot surface is a measure of convective heat transfer coefficient at the surface. Higher values of Nu indicate higher heat transfer rate from the hot surface. The local Nusselt number from the isothermal top face of the object is computed as, $Nu(Y) = -d\theta/dx\big|_{TopFace}$ and the average Nusselt number is calculated as, $\overline{Nu} = 1/W\int_{l_1}^{l_2} Nu(Y)\,dY$, where $W=l_2-l_1$ is the face width of the top face of the object as in Figure 1. Similarly, the average Nusselt number of left and right vertical sides of the object are computed. Now, taking the average of three sides will give the average heat transfer from the object. An index of the performance of the overall heating process of fluid is defined in terms of the heating efficiency, ε [9], which is defined as the ratio of the net heat energy flux through the inlet and outlet to the heat energy influx, i.e., $\varepsilon = \int_{A_{in+out}} \overline{\theta} v.ndA \Big/ \int_{A_{in}} \theta v.ndA$ where **v** is the velocity vector and **n** is the outward-drawn unit normal vector. Defining the average inlet and outlet temperatures as, $\overline{\theta}_{in} = \int_{A_{in}} \theta v.ndA \Big/ \int_{A_{in}} v.ndA$ and $\overline{\theta}_{out} = \int_{A_{out}} \theta v.ndA \Big/ \int_{A_{out}} v.ndA$ and noting that for steady state $\int_{A_{in}} v.ndA = \int_{A_{out}} v.ndA$ the heating efficiency is given by [9], $\varepsilon = 1 - \overline{\theta}_{out}/\overline{\theta}_{in}$.

## NUMERICAL MODELING

The conservation equations for mass, momentum, and energy for the two-dimensional, steady, and laminar flow. All the physical properties of the fluid, $\mu$, k, and $C_p$, are considered constant except density, in the buoyancy term, which follows the Boussinesq approximation. In the energy equation, the effects of compressibility and viscous dissipation is neglected.

Continuity equation

$$\frac{\partial u}{\partial x} + \frac{\partial v}{\partial y} = 0. \tag{1}$$

Navier-Stokes equations

$$u\frac{\partial u}{\partial x} + v\frac{\partial u}{\partial y} = -\frac{1}{\rho}\frac{\partial p}{\partial x} + \nu\left(\frac{\partial^2 u}{\partial x^2} + \frac{\partial^2 u}{\partial y^2}\right) \tag{2}$$

$$u\frac{\partial v}{\partial x} + v\frac{\partial v}{\partial y} = -\frac{1}{\rho}\frac{\partial p}{\partial y} + \nu\left(\frac{\partial^2 v}{\partial x^2} + \frac{\partial^2 v}{\partial y^2}\right) + g\beta(T_{obj} - T_\infty) \tag{3}$$

Energy equation

$$u\frac{\partial T}{\partial x} + v\frac{\partial T}{\partial y} = \alpha\left(\frac{\partial^2 T}{\partial x^2} + \frac{\partial^2 T}{\partial y^2}\right) \tag{4}$$

The above equations are converted into a non-dimensional form considering the following dimensionless quantities:

$$X = \frac{x}{W};\quad Y = \frac{y}{W};\qquad U = \frac{uW}{\alpha};\quad V = \frac{vW}{\alpha};$$

$$\theta(x,y) = \frac{T(x,y) - T_\infty}{T_{obj} - T_\infty}$$

Now, putting this value in equation (1), (2), (3) and (4), we get the normalized forms of these equations are as follows,

$$\frac{\partial u}{\partial x} + \frac{\partial v}{\partial y} = 0 \tag{5}$$

$$u\frac{\partial u}{\partial x} + v\frac{\partial u}{\partial y} = -\frac{1}{2}\frac{\partial p}{\partial x} + \Pr\left(\frac{\partial^2 u}{\partial x^2} + \frac{\partial^2 u}{\partial y^2}\right) \tag{6}$$

$$u\frac{\partial v}{\partial x} + v\frac{\partial v}{\partial y} = -\frac{1}{2}\frac{\partial p}{\partial y} + \Pr\left(\frac{\partial^2 v}{\partial x^2} + \frac{\partial^2 v}{\partial y^2}\right) + Ra.\Pr\theta \tag{7}$$

and

$$u\frac{\partial \theta}{\partial x} + v\frac{\partial \theta}{\partial y} = \left(\frac{\partial^2 \theta}{\partial x^2} + \frac{\partial^2 \theta}{\partial y^2}\right) \tag{8}$$

## BOUNDARY CONDITIONS

### Boundary Conditions at the Bottom Wall

Since the Velocity Component, u and v both are zero at the wall. We know that the velocity components are:

$u = \frac{\partial \psi}{\partial y}$ and $v = -\frac{\partial \psi}{\partial x}$ Applying no-slip conditions, u=0 and v=0, stream function ψ=constant. The vorticity at the bottom wall is prescribed by the constant $\omega = \frac{0.05\,\mathrm{Re}}{2}$ and the bottom wall is assumed to be heated one-third of the heated object, that is, θ=0.3.

**Boundary Conditions at Left and Right Boundaries**

Gradients of variables are assumed to be zero at the left and right boundaries are as,

$$\frac{\partial u}{\partial x} = 0; \frac{\partial v}{\partial x} = 0; \frac{\partial \psi}{\partial x} = 0; \frac{\partial \omega}{\partial x} = 0; \frac{\partial \theta}{\partial x} = 0;$$

**Boundary Conditions at object**

At the object, for no-slip conditions, u=0 and v=0, Stream function ψ= constant. The vorticity at the object boundary is prescribed by the constant, $\omega = \frac{0.05\,\mathrm{Re}}{2}$. The object is assumed to be heated. So, the temperature field associated with the object boundary is: θ=1.0.

**Boundary Conditions at Top Boundary**:

Gradients of variables and u-component of velocity are assumed to be zero at the top boundary as,

$$u = 0; \frac{\partial v}{\partial x} = 0; \frac{\partial \psi}{\partial x} = 0; \frac{\partial \omega}{\partial x} = 0; \frac{\partial \theta}{\partial x} = 0;$$

## RESULT AND DISCUSSION

The governing non-dimensional partial differential equations along with proper boundary conditions have been solved to get stream function, vorticies, velocities and temperatures at every nodal points in the computational domain. Computational domain is shown in the Fig. 1.

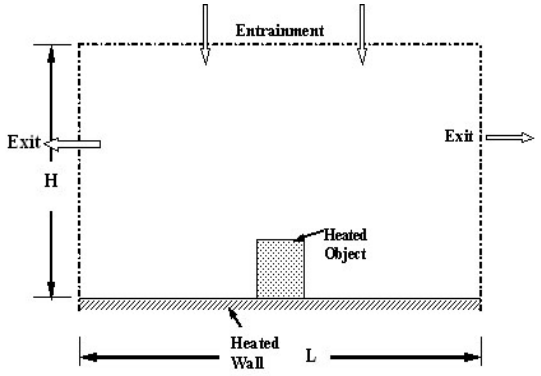


Figure 1. Computational Domain

The length of the computational domain is L=12 and height H=5. The top face width of the object W=1.0 and the height of the object $H_{obj}$=0.34. Uniform grid is specified in the axial direction and non-uniform grid is specified in the vertical direction. Grid independency test has been done, but no improved result is obtained after more fine grids than 50 × 50, which is shown in the Fig. 2. The maximum error is obtained as $10^{-6}$ based on stream function.

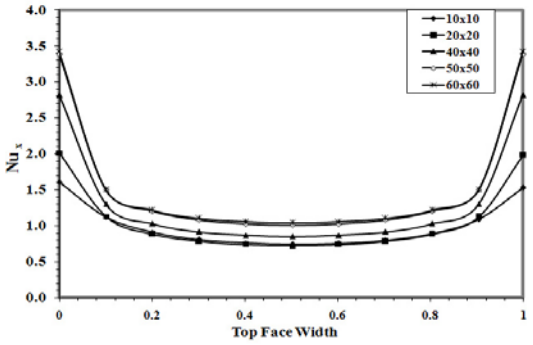


Figure 2. Grid Sensitivity Test

Figure 3 shows, the stream function contours at Ra=50. It is observed that the fluid is flowing over the heated body and transferring heat from the heated body. Small vorticies are observed at top and adjacent to the heated body.

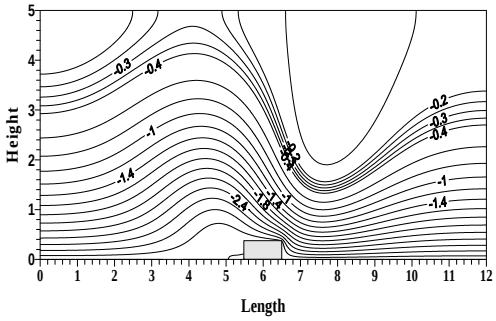


Figure 3. Stream Function at Ra=50.

Figure 4 shows the velocity vector at Ra=50. It is observed that the fluid is flowing over the heated body becomes heated and goes upward. At the same time cold entrainment is added to the main flow stream. Fluid is coming from left and top of the computational domain and going out from right boundary and top boundary.

Figure 5 shows the temperature contours at Ra=50. It is observed that the cold fluid is coming as entrainment and mixed with the heated fluid flowing towards the heated object and takes heat, becomes lighter and goes upward.

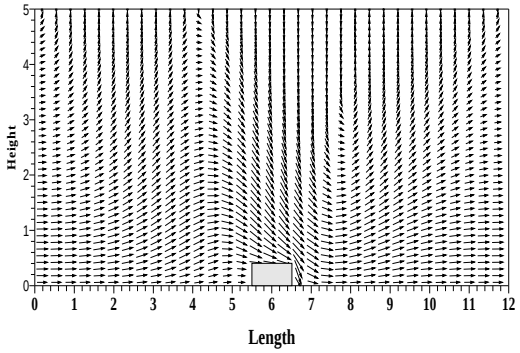


Figure 4. Velocity vector at Ra=50.

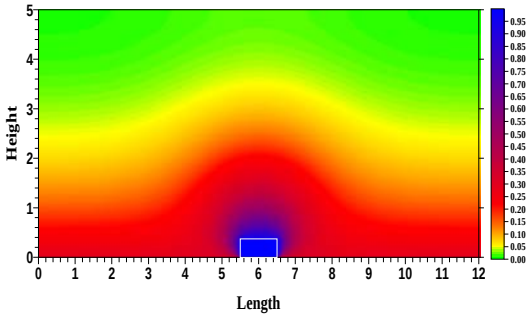


Figure 5. Contour of Temperature at Ra=50.

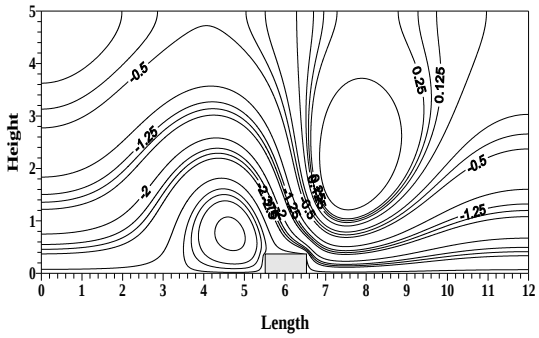


Figure 6. Stream Function at Ra=100.

Figure 6 shows the stream function at Ra=100. It is observed that the two separate and distinct vorticies are formed near the heated object. Cold fluid entering into the domain becomes heated and goes upward. In this way heat is transferred to the surrounding.

Figure 7 shows the velocity vector at Ra=100. Two distinct vorticies are observed in the flow field. Cold fluid is coming from the surrounding mixed with the heated fluid and goes back to the surrounding.

Figure 8 shows the temperature contours at Ra=100. It is observed that the cold fluid region gradually narrow and heated fluid spreads over the flow field. The fluid flowing towards the heated object and takes heat, becomes lighter and goes upward.

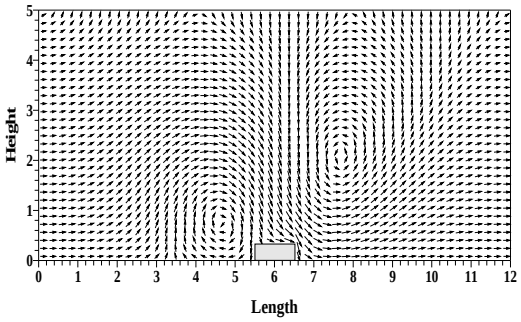


Figure 7. Velocity Vector at Ra=100.

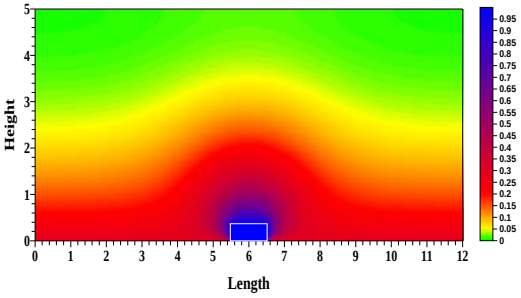


Figure 8. Contour of Temperature at Ra=100.

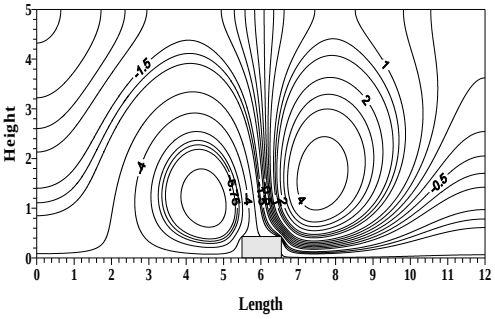


Figure 9. Stream Function at Ra=300.

Figure 9 shows the stream function at Ra=300. It is observed that the two separate and distinct vorticies are formed near the heated object. Cold fluid entering into the domain becomes heated and goes upward. In this way heat is transferred to the surrounding.

Figure 10 shows the velocity vector at Ra=300. Two distinct and sharp vorticies are observed in the flow field. The magnitude of fluid velocities increased, mixed quickly and goes back to the surrounding.

Figure 11 shows the temperature contours at Ra=300. It is observed that the cold fluid region becomes more narrow and heated fluid spreads over the flow field. The fluid flowing towards the heated

object and takes heat, becomes lighter and goes upward.

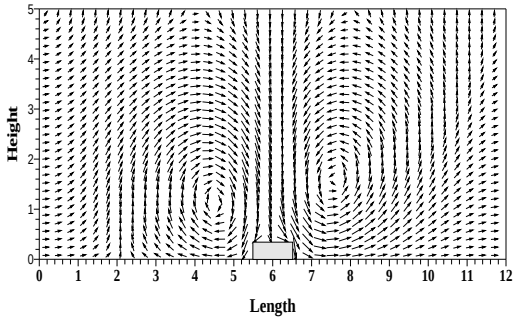


Figure 10. Velocity Vector at Ra=300.

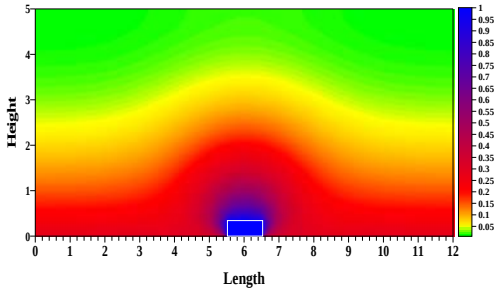


Figure 11. Contour of Temperature at Ra=300.

Figure 12 shows that the average Nusselts number for the range of Ra=10 to 600. It is observed that the average Nusselt number varies very little that is, almost constant. Deviation is not considerable.

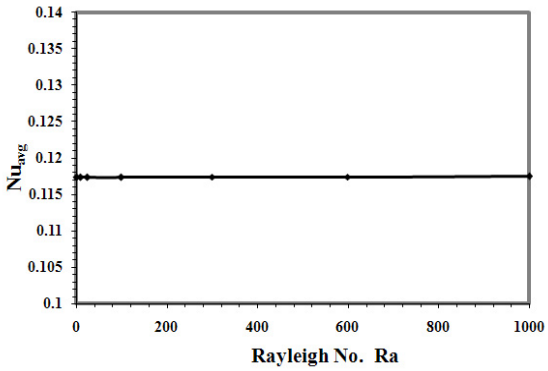


Figure 12. Average Nusselts number at different Ra.

Figure 13 shows that the heating efficiency for the range of Ra=10 to 600. It is observed that the heating efficiency sharply varies within the lower values of Rayleigh number but at higher values of Rayleigh number heating efficiency remains almost constant

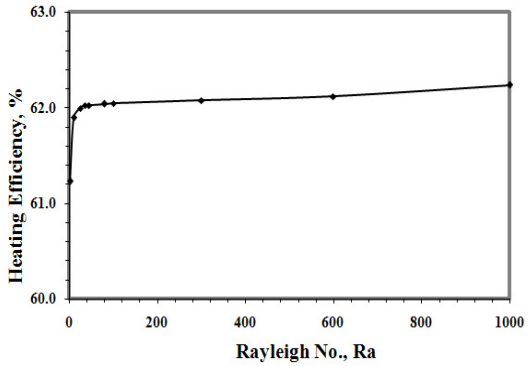


Figure 13. Heating Efficiency at different Ra.

## CONCLUSIONS

This investigation led to several conclusions:

1. The vorticies are formed with the increase of Rayleigh Number and become sharp.
2. The temperature spreads gradually with the increase of Rayleigh Number.
3. The average Nusselt Number remains almost constant for the range of Rayleigh Number investigated.
4. The heating efficiency changes sharply at low Rayleigh Number but Ra=35 and more the heating efficiency remains almost constant.

## NOMENCLATURE

| Symbols | Description |
|---|---|
| H | Height of the Domain |
| L | Length of the Domain |
| $H_{obj}$ | Filament Height |
| k | Thermal conductivity of the fluid |
| Nu | Nusselt Number |
| p | Pressure of the flowing fluid |
| Pr | Prandtl Number, $\Pr = \frac{\nu}{\alpha}$ |
| Gr | Grashof number, $Gr = \frac{g\beta\Delta\theta W^3}{\nu^2}$ |
| T(x,y) | Local fluid temperature |
| $U$ , $V$ | Dimensionless velocity components, |

$U = \frac{uW}{\alpha}$, $V = \frac{vW}{\alpha}$

x, y Cartesian coordinates

X, Y Dimensionless Cartesian coordinates, $\frac{x}{W}, \frac{y}{W}$

ρ Density of fluid

ν Kinematics viscosity of fluid

ω Vorticity

ω* Dimensionless Vorticity, $\frac{\omega}{\omega_o}$

θ $= \frac{T - T_\infty}{T_{obj} - T_\infty}$

ψ Stream function

$\psi_o$ Initial value of Stream function

ψ* Dimensionless Stream function, $\frac{\psi}{\psi_o}$

W Top face width of the object

**REFERENCES**

[1] Salam, S. A. and Ahmed, K. H., "Natural Convection Heat Transfer in a Differentially Heated Square Enclosure with a Heat Generating-Conducting Circular Cylinder at Different Diagonal Locations." Proceeding of 6th International Advanced Technologies Symposium (IATS'11), 16-18 May 2011, Elazığ, Turkey , pp.13-19.

[2] Oh, J. Ha, M. and Kim, K. "Numerical study of heat transfer and flow of natural convection in an enclosure with a heat generating conducting body", Numerical Heat Transfer, Part A ,Vol. 31, 1997, pp.289-304.

[3] Roychowdhury, D., Das, S. and Sundararajan, T. "Numerical simulation of natural convective heat transfer and fluid flow around a heated cylinder inside an enclosure", International Journal of Heat and Mass Transfer, Vol. 38, 2002, pp.565–576.

[4] Arnab, K. and Amaresh, D. "A numerical study of natural convection around a square, horizontal, heated cylinder placed in an enclosure.", International Journal of Heat and Mass Transfer, Vol. 49, 2006, pp.4608-4623.

[5] Jami, M., Mezrhab, A., Bouzidi, M. and Lallemand, P. "Lattice Boltzmann method applied to the laminar natural convection in an enclosure with a heat-generating cylinder conducting body., Graduate Student Association Research Fair, University of Nevada , Reno, 2006, pp.1–20.

[6] Sidik, N. and Rahman, M., "Mesoscale investigation of natural convection heat transfer from a heated cylinder inside square enclosure.", European Journal of Scientific Research, Vol. 38, No. 1, 2009, pp.45-56.

[7] Hussain, S. and Hussein, A. "Numerical investigation of natural convection phenomena in a uniformly heated circular cylinder immersed in square enclosure filled with air at different vertical locations", International Communications in Heat and Mass Transfer, Vol.37, 2010, pp.1115–1126.

[8] Bailey, R. T. , Mitchell, J. W. and Beckman, W. A. "Convective Heat Transfer From a Desert Surface." Journal of Heat Transfer, February 1975,Volume 97, Issue 1, pp.104-109.

[9] Singh S., and Sharif, M. A. R.,"Mixed Convective Cooling of a Rectangular Cavity with Inlet and Exit Openings on Differentially Heated Side Walls", Numerical Heat Transfer, Part A, Vol 44 (2003), pp.615-637.